

Quantum annealing and nonequilibrium dynamics of Floquet Chern insulators

Lorenzo Privitera¹ and Giuseppe E. Santoro^{1,2,3}

¹SISSA, Via Bonomea 265, I-34136 Trieste, Italy

²CNR-IOM Democritos National Simulation Center, Via Bonomea 265, I-34136 Trieste, Italy

³International Centre for Theoretical Physics (ICTP), P.O. Box 586, I-34014 Trieste, Italy

(Received 15 September 2015; revised manuscript received 19 May 2016; published 15 June 2016)

Inducing topological transitions by a time-periodic perturbation offers a route to controlling the properties of materials. Here, we show that the adiabatic preparation of a nontrivial state involves a selective population of edge states, due to exponentially small gaps preventing adiabaticity. We illustrate this by studying graphenelike ribbons with hopping's phases of slowly increasing amplitude, as, e.g., for a circularly polarized laser slowly turned on. The induced currents have large periodic oscillations, but flow solely at the edges upon time averaging, and can be controlled by focusing the laser on either edge. The bulk undergoes a nonequilibrium topological transition, as signaled by a local Hall conductivity, the Chern marker introduced by Bianco and Resta in equilibrium. The breakdown of this adiabatic picture in the presence of intraband resonances is discussed.

DOI: 10.1103/PhysRevB.93.241406

Introduction. Recent experiments [1] have mapped the phase diagram of the Haldane model [2], a prototypical Chern insulator, by driving ultracold fermionic atoms in an optical honeycomb lattice periodically modulated in time. Since the early suggestion by Oka and Aoki [3] for a photovoltaic Hall effect in graphene, theoretical research aimed at studying topological transitions induced by an external periodic perturbation—the so-called *Floquet topological insulators* [4]—has been intense [5–19]. Preparing a topologically nontrivial Floquet insulator, out of a standard band insulator, requires passing through a phase transition point, where the bulk energy gap momentarily closes and edge states start crossing it. It is usually assumed that this can be done by keeping the system arbitrarily close to its Floquet “ground state” (GS), a concept which we will clarify later on, provided the strength of the periodic perturbation is ramped up in an adiabatic way [7,20,21]—realizing a generalized form of quantum annealing (QA) [22–25]. In this Rapid Communication we study the QA dynamics of the Haldane model across its topological transition, and that of periodically driven graphenelike ribbons, e.g., irradiated by a circularly polarized laser. We find that the topological transition comes with an ingredient that makes it different from the Kibble-Zurek (KZ) paradigm [26,27] describing the crossing of ordinary critical points [25,28,29]: an exponentially small Landau-Zener (LZ) [30,31] avoided-crossing gap between edge states, which forbids edge-state electrons from adiabatically following the GS, no matter how slowly the critical point is crossed. The peculiarity of this QA dynamics is reflected in nonequilibrium currents flowing at the edges, which could be controlled, e.g., by a laser focusing on the edges. We also show how the change in the topology of the nonequilibrium state is effectively signaled by the dynamical counterpart of a local Chern marker, introduced by Bianco and Resta [32] as an indicator of an equilibrium nontrivial bulk topology.

Model and idea. Graphenelike systems display remarkable properties associated with the pseudospin- $\frac{1}{2}$ \mathcal{A} - \mathcal{B} sublattice degree of freedom of the honeycomb lattice, with relativistic Dirac cones sitting at the two corners $\mathbf{K}_{\pm} = (\frac{2\pi}{\sqrt{3}a}, \pm \frac{2\pi}{3a})$ — a being the lattice constant—of the hexagonal Brillouin zone

(BZ), when inversion symmetry (IS) and time-reversal symmetry (TRS) are unbroken. A minimal single-orbital tight-binding model, allowing for a time dependence in the nearest-neighbor (NN) hopping phase and in the on-site energy, is given by the following Hamiltonian (omitting spin indices),

$$\hat{H}(t) = t_1 \sum_{(ij)} e^{-i\Phi_{ij}(t)} \hat{c}_j^{\dagger} \hat{c}_i + \Delta_{AB}(t) \sum_i (-1)^i \hat{c}_i^{\dagger} \hat{c}_i, \quad (1)$$

where \hat{c}_i^{\dagger} creates a particle at site i , (ij) denotes sums over NN, and $(-1)^i = +1/-1$ on \mathcal{A}/\mathcal{B} . Δ_{AB} controls IS, opens up a trivial equilibrium gap at the Dirac points, and is in principle controllable versus time in optical lattice experiments [1]. The phases $\Phi_{ij}(t)$ —generally breaking TRS—may result from a time-periodic modulation of the optical lattice in the neutral cold-atom experiments [1], or from the Peierls' substitution minimal coupling of the electrons with the (classical) electromagnetic field of a laser $\Phi_{ij}(t) = \frac{e}{\hbar c} \int_i^j d\mathbf{l} \cdot \mathbf{A}(\mathbf{x}, t)$. With the latter realization in mind, we take the field monochromatic and described by a vector potential $\mathbf{A}(\mathbf{x}, t) = A_0(\mathbf{x}, t)[\hat{\mathbf{x}} \sin(\omega t) + \hat{\mathbf{y}} \sin(\omega t - \varphi)]$, where φ describes a general elliptical polarization of the laser and $A_0(\mathbf{x}, t)$ is a smooth function of space and time.

For a circularly polarized ($\varphi = \pm\pi/2$) spatially uniform laser [3,7,16,19], $\Phi_{ij}(t) = \lambda(t) \sin(\omega t + \phi_{ij})$, with $\phi_{ij} = (\pm\frac{\pi}{3}, \mp\frac{\pi}{3}, \pi)$ along the three NN directions ($\mathbf{d}_1, \mathbf{d}_2, \mathbf{d}_3$) connecting an \mathcal{A} site to its NN \mathcal{B} sites, and $\lambda(t) = \frac{ed}{\hbar c} A_0(t)$, d being the NN distance. If the frequency ω is larger than the unperturbed bandwidth $W = 6|t_1|$, and $\lambda(t)$ and $\Delta_{AB}(t)$ are nearly constant during a period $\tau = 2\pi/\omega$, the resulting Floquet evolution operator $\hat{U}(\tau, 0) = e^{-i\hat{H}^F \tau/\hbar}$ has an effective Floquet Hamiltonian \hat{H}^F approximately given by a Haldane model \hat{H}_H with flux $\phi_H = \pm\frac{\pi}{2}$, the same on-site difference Δ_{AB} , and hoppings renormalized by Bessel functions: $t_1 \rightarrow t_1 J_0(\lambda)$, $t_2 = -\sqrt{3}[t_1 J_1(\lambda)]^2/(\hbar\omega)$ [7]. As the amplitude $\lambda(t)$ is slowly turned on—and/or $\Delta_{AB}(t)$ is slowly decreased to 0—we effectively drive the Haldane model $\hat{H}_H(t)$ across its equilibrium critical point $(\Delta_{AB}/t_2)_c = 3\sqrt{3}$ [2]. In what follows, we study zigzag strips with open boundary conditions (OBCs) and N_x sites in the x direction, and periodic BC (PBC) along y [see the inset in Fig. 2(b')]. For each of the

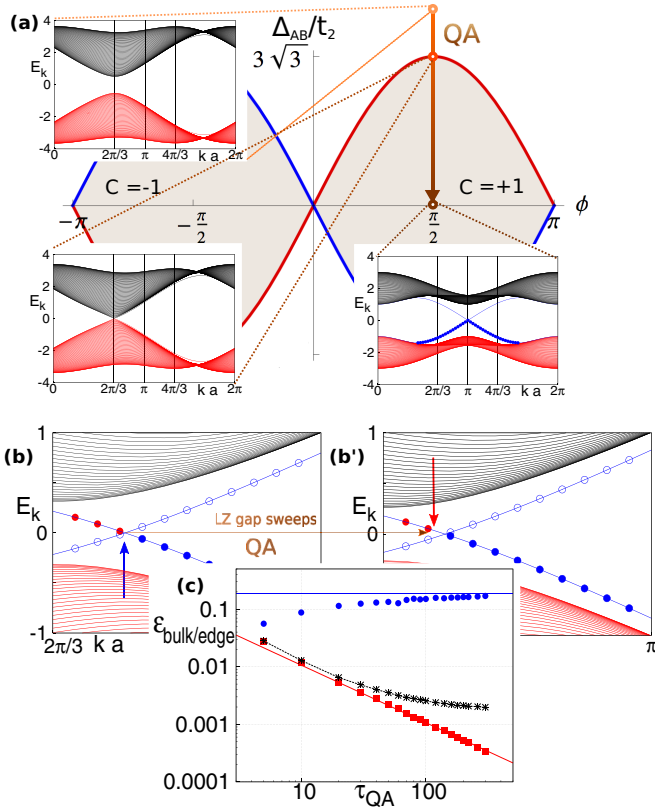


FIG. 1. (a) Phase diagram of the Haldane model, with three representative zigzag strip spectra, along the path of the QA evolution (arrow). (b), (b') The mechanism by which right-edge states get selectively populated as the exponentially small LZ gap sweeps to larger values of k during the QA evolution. The (equilibrium) edge states shown refer to $\Delta_{AB}/t_2 = 2.5$ [for (b)] and $\Delta_{AB}/t_2 = 2.4$ [for (b')]. Solid/open circles denote occupied/empty edge states. The blue vertical arrow in (b) points to an occupied right-edge electron that remains occupied [red vertical arrow in (b')] after the Landau-Zener event. (c) Residual energy (stars), separated into bulk (squares) and edge (circles) contributions, vs the annealing time τ_{QA} . Here, data with $L = N_x = N_y = 6n$ from 18 to 102 were used to get $\varepsilon_{\text{bulk/edge}}$ for each τ_{QA} .

N_y y -momenta k , the single-particle Hamiltonian is a $N_x \times N_x$ matrix $\mathbb{H}(k, t)$ whose Schrödinger dynamics is numerically integrated with a fourth-order Runge-Kutta method, the initial state $|\Psi(0)\rangle$ being the Slater determinant GS of $\hat{H}(0)$ at half filling [33].

As a warmup, let us first consider a QA of the Haldane model. Its phase diagram [2], Δ_{AB}/t_2 vs ϕ_H , is shown in Fig. 1(a), the shaded regions denoting the topologically nontrivial phases with Chern number $C = \pm 1$. In the insets, we show three zigzag spectra at $\phi_H = \frac{\pi}{2}$: a trivial insulator with $\Delta_{AB}/t_2 = 4\sqrt{3}$, the critical point $(\Delta_{AB}/t_2)_c = 3\sqrt{3}$, and the IS-symmetric point with $\Delta_{AB} = 0$. Edge states cross the bulk gap in the nontrivial phase; the crossing k point between the two branches moves from the bulk-projected Dirac point $K_+ = 2\pi/(3a)$ towards $K_f = \pi/a$ as Δ_{AB}/t_2 decreases from $(\Delta_{AB}/t_2)_c$ to $\Delta_{AB} = 0$. Actually, this is an *avoided-crossing* LZ point, with an *exponentially small* gap $\sim e^{-L_x/\xi}$, where L_x

is the strip width and ξ the localization length of the edge states, separating the two quasidegenerate edge states. Consider the evolution denoted by the arrow in Fig. 1(a): Δ_{AB}/t_2 starts from $4\sqrt{3}$ and ends in 0 in a time τ_{QA} . In the initial part of the evolution, the Dirac-point (bulk) gap $\Delta_{K_{\pm}}$ closes at criticality as $\Delta_{K_{\pm}} \sim 1/L$, resulting in a standard KZ [26,27] nonadiabatic excitation of electrons into the conduction band [25]. In two dimensions (2D), the critical exponents $\nu = 1$, $z = 1$ should lead to a residual energy $E_{\text{res}}(t) = \langle \Psi(t) | \hat{H}(t) | \Psi(t) \rangle - E_{\text{gs}}(t)$, $E_{\text{gs}}(t)$ being the instantaneous GS energy, scaling as $\varepsilon_{\text{res}} = E_{\text{res}}(t = \tau_{QA})/L^2 \sim \tau_{QA}^{-1}$. The bare data for ε_{res} [stars in Fig. 1(c)] depart from this KZ scaling, due to a mechanism of selective edge-state excitation, which we now discuss. Consider the right-edge electron sitting immediately to the right of the LZ gap in Fig. 1(b) (here we have only $N_y = 72$ k points for clarity of illustration): As the LZ gap sweeps towards larger k , it will be *unable to follow the ground state* due to the exponentially small LZ gap, and will remain in the right-edge band [see Fig. 1(b')], but *excited*, since the equilibrium lowest-energy state sits in the left-edge band. In essence, *there cannot be any LZ tunneling across the opposite edges of the sample*. Hence, left-edge states remain, one after the other, selectively unoccupied. If we separate the contributions due to bulk and edges, $E_{\text{res}} = \varepsilon_{\text{bulk}}L^2 + \varepsilon_{\text{edge}}L$, we find that $\varepsilon_{\text{bulk}} \sim \tau_{QA}^{-1}$ [solid squares in Fig. 1(c)], while $\varepsilon_{\text{edge}}$ (solid circles) slowly increases, approaching the value $\varepsilon_{\text{edge}}^{\text{LZ}} = \int_{K_+}^{K_f} \frac{dk}{2\pi} [E_{k,+} - E_{k,-}]$, where $E_{k,+/-}$ are the right/left final edge bands. Starting the QA evolution from negative Δ_{AB}/t_2 , or having $\phi_H = -\frac{\pi}{2}$, swaps the role of right and left, and of the two Dirac points.

Adiabatic Floquet results. We now return to our Floquet QA, Eq. (1), with a circularly polarized driving. We performed an “adiabatic” linear turning on of $\lambda(t) = (t/\tau_{QA})\lambda_f$ for a time $\tau_{QA} = n_{QA}\tau$, followed by an evolution with constant λ_f for $\tau_f = n_f\tau$ (with $\tau = 2\pi/\omega$). We considered both a time-independent Δ_{AB} , and a $\Delta_{AB}(t)$ switched off to 0 during the annealing of $\lambda(t)$ (physically possible in the cold-atom realization). In principle, $\Delta_{AB} = 0$ in graphene, but the initial zigzag edge states would be pathological symmetric/antisymmetric combinations of left-right wave functions [34]. Hence, to describe graphene we include a very small $\Delta_{AB} = 0^{\pm}$ whose value is not crucial (only the sign matters); the results turn out to be identical to evolutions in which $\Delta_{AB}(t)$ is switched off to 0. A generalized adiabatic theorem holds for Floquet systems [7,20,21,35,36]: A Floquet state $|\psi_{\alpha}[\lambda(0)]\rangle$ evolves remaining close to the instantaneous Floquet state $|\psi_{\alpha}[\lambda(t)]\rangle$ for sufficiently slow variations of the driving amplitude $\lambda(t)$, compared to the gaps from neighboring states $\min_{m \in \mathbb{Z}} (|\epsilon_{\alpha} - \epsilon_{\beta} + m\hbar\omega|)$. For $\hbar\omega > W$, the standard Floquet BZ $[-\hbar\omega/2, \hbar\omega/2]$ is such that the initial Slater determinant $|\Psi(0)\rangle$ coincides with the *Floquet ground state* $|\Psi_{\text{FGS}}[\lambda(0) = 0]\rangle$: All negative quasienergies, in $[-\hbar\omega/2, 0)$, are occupied, and the positive ones are empty. The only relevant gap for the adiabatic Floquet dynamics [20,21] is that at the Dirac points. A slow increase of λ will reproduce the QA of the Haldane case, as we verified by monitoring the occupations $n_{k,\alpha}$ of the instantaneous single-particle Floquet modes $|\phi_{k,\alpha}\rangle$ [33]: The state $|\Psi(\tau_{QA})\rangle$ after the annealing is “close” to $|\Psi_{\text{FGS}}[\lambda(\tau_{QA})]\rangle$, apart from bulk KZ excitations

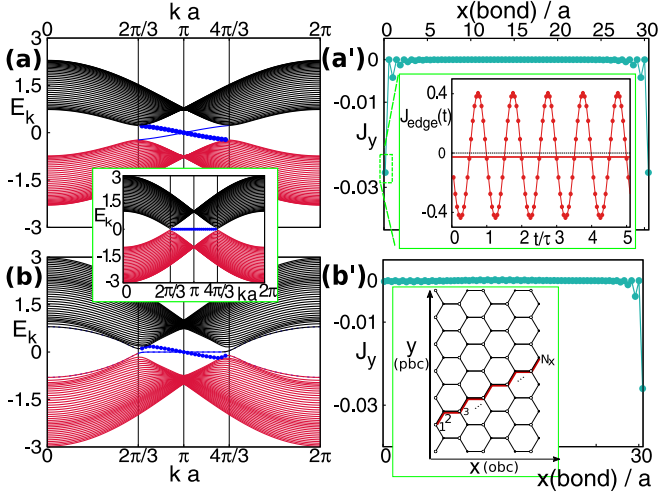


FIG. 2. (a) Final Floquet quasienergy bands for a uniform driving with $\phi = -\pi/2$, $\hbar\omega = 7|t_1| > W$, $\Delta_{AB} = 10^{-3}|t_1|$ (effectively representing graphene), and $\lambda(t)$ linearly ramped up to $\lambda_f = 1$ in $\tau_{QA} = 100\tau$, with $\tau = 2\pi/\omega$. Here, the topological transition occurs at $\lambda_{cr} \approx 0$. Valence states (in red) are filled, conduction states (in black) empty. Solid circles denote occupied edge states. Inset: The initial graphene spectrum at $\lambda(0) = 0$. (a') Time-averaged bond currents calculated with a periodic evolution at constant λ_f for $\tau_f = 100\tau$. The inset shows the large intraperiod oscillations. (b), (b') Same as (a) and (a') for an inhomogeneous driving focused on the right edge ($x_c = L_x$) of width $\sigma = 0.4L_x$. In the inset, a sketch of the zigzag strip.

near the Dirac points, and the previously discussed selective excitation of edge states [see Fig. 2(a)].

The dynamics of the Hall current is interesting. As customary, in a Laughlin cylinder geometry the total current in the y direction is given by $\hat{J}_y = \frac{1}{\hbar} \frac{\partial \hat{H}}{\partial \kappa_y} \Big|_{\kappa_y=0}$, where $\kappa_y = \frac{2\pi}{N_y a} \frac{\Phi_L}{\phi_0}$ is related to the flux Φ_L , piercing the PBC cylinder along the x axis, and ϕ_0 is the flux quantum [37]. With PBC along y , we can write $\hat{H}(t) = \sum_k^{BZ_y} \sum_{i,i'} \mathbb{H}_{i,i'}(k,t) \hat{c}_{i,k}^\dagger \hat{c}_{i',k}$, where $\mathbb{H}(k,t)$ is the k -resolved strip Hamiltonian and $\hat{c}_{i,k}^\dagger$ creates an electron of momentum k at site i along the zigzag line sketched in Fig. 2(b'). Hence, bond-resolved y currents are $J_{i,i+1}(t) = \langle \Psi(t) | \sum_k^{BZ_y} \mathbb{J}_{i,i+1}(k,t) \hat{c}_{i,k}^\dagger \hat{c}_{i+1,k} | \Psi(t) \rangle$ with $\mathbb{J} = \frac{1}{\hbar} \frac{\partial \mathbb{H}}{\partial \kappa_y} \Big|_{\kappa_y=0}$. The circles in Fig. 2(a') denote the time average of $J_{i,i+1}(t)$ during the constant- λ_f evolution, $[J_{i,i+1}]_{av} = \frac{1}{n_f \tau} \int_{\tau_{QA}}^{\tau_{QA} + n_f \tau} dt J_{i,i+1}(t)$. Currents are concentrated at the edges, but with large periodic oscillations, shown in the inset: The stroboscopic averages are not representative of the true time averages [33]. Notice that the edge currents have left/right symmetry, while one would naively expect currents only on the edge which is selectively occupied by the out-of-equilibrium dynamics (the right edge, for Fig. 2). This behavior originates from specific symmetries—previously noted in equilibrium for the Haldane model at $\phi_H = \pm\pi/2$ [15,18]—whereby the GS value of \hat{J}_y is zero everywhere due to an exact compensation between currents due to edge states and edge-current contributions due to bulk states. Since the out-of-equilibrium dynamics brings a lack of current-carrying edge

states [at left, in Fig. 2(a)], the corresponding bulk contribution is uncompensated and gives rise to a left-flowing current of the same sign and amplitude as that at the right edge. This left/right symmetry can be removed by a space inhomogeneity of the perturbation, e.g., a laser focused off center. Here, we find it expedient to retain translational invariance along y , assuming a y -independent Gaussian modulation amplitude $A_0(\mathbf{x}, t) = A_0(t) e^{-(x-x_c)^2/2\sigma^2}$, where x_c is the focus center, and σ the beam width. All the previous results remain valid for a central focusing, $x_c = L_x/2$, provided σ is not too small ($\sigma \gtrsim 0.4L_x$). But the interesting feature is the ability to control the edge current to flow on either edge of the sample by moving the focus off-center. Figure 2(b) illustrates the final Floquet quasienergy bands when the laser is focused on the right edge ($x_c = L_x$), with $\sigma = 0.4L_x$. Notice that only the irradiated right-edge states show a k dispersion: Unirradiated left-edge states stay flat and carry no current. Nonequilibrium currents flow only at the irradiated edge [see Fig. 2(b')].

It is interesting to address the issue of an “indicator” of nontrivial topology in a nonequilibrium translationally noninvariant setting. For translationally invariant systems (with PBC), it was shown that the usual Chern number \mathcal{C} is conserved during a unitary evolution [14,18]: It does not “signal” the topological transition. However, since for $\hbar\omega > W$ the nontrivial final bulk states are adiabatically populated in a controlled way, we would expect to be able to “see” the topological transition by looking only at the “bulk” of the sample. We find that the local Chern marker $\mathcal{C}(\mathbf{r})$, introduced in Ref. [32] at equilibrium, essentially a local measure of the Hall conductivity, works also in our nonequilibrium context: It signals if the sample bulk is locally a topologically nontrivial insulator, $\mathcal{C}(\mathbf{r}) \sim \pm 1$. $\mathcal{C}(\mathbf{r})$ can be expressed as a physically appealing commutator of position operators [32,33],

$$\mathcal{C}(\mathbf{r}, t) = -2\pi i \langle \mathbf{r} | [\hat{x}_{\mathcal{P}(t)}, \hat{y}_{\mathcal{P}(t)}] | \mathbf{r} \rangle. \quad (2)$$

Here, $\hat{x}_{\mathcal{P}} = \mathcal{P} \hat{x} \mathcal{P}$ and $\hat{y}_{\mathcal{P}} = \mathcal{P} \hat{y} \mathcal{P}$ are position operators projected on the occupied states, $\mathcal{P}(t)$ being the projector on the time-evolved Slater determinant $|\Psi(t)\rangle$. Figure 3 illustrates the dynamics of $\mathcal{C}(\mathbf{r}, t)$, averaged over a central “bulk” portion of the sample, $C_{\text{bulk}}(t) = N_{\text{bulk}}^{-1} \sum_{\mathbf{r} \in \text{bulk}} \mathcal{C}(\mathbf{r}, t)$ as the system evolves from a trivial insulator at $\lambda = 0$, towards the nontrivial point with $\lambda_f = 1$. Upon time averaging the oscillations after τ_{QA} [33], we obtain a quantity $C_{\text{bulk}}^{\text{av}}(L, \tau_{QA}) = \frac{1}{n_f \tau} \int_{\tau_{QA}}^{\tau_{QA} + n_f \tau} dt C_{\text{bulk}}(t)$ approaching the correct integer value 1 as $\tau_{QA} \rightarrow \infty$ and $L \rightarrow \infty$ (see insets in Fig. 3).

When $\hbar\omega$ is smaller than the bandwidth W , intraband resonances between valence states at ϵ_α and conduction ones at $\epsilon_\beta \approx \epsilon_\alpha + \hbar\omega$ change the physics completely, breaking the Floquet adiabatic picture. The whole crux is, in essence, that the starting point at $\lambda(0) = 0$ —the usual Slater determinant $|\Psi(0)\rangle \neq |\Psi_{\text{FGS}}[\lambda(0) = 0]\rangle$, for any choice of the Floquet BZ: Upon folding the original $[-W/2, W/2]$ spectrum in, e.g., $[-\hbar\omega/2, \hbar\omega/2]$, we see that the lower Floquet quasienergy band is only partially filled, with empty conduction-band-originated states intermixed with filled valence-band ones. These filled-empty pairs with small Floquet gaps [20,21] $\min_{m \in \mathbb{Z}} (|\epsilon_\alpha - \epsilon_\beta + m\hbar\omega|)$ lead to a proliferation of bulk LZ events as $\lambda(t)$ is ramped up, with a complex redistribution

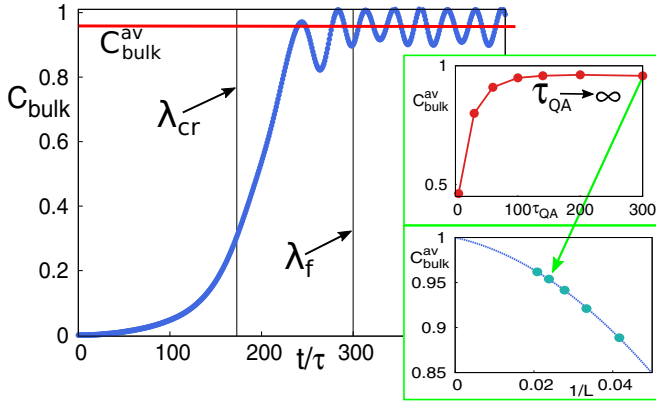


FIG. 3. The bulk average $C_{\text{bulk}}(t)$ of the local Chern marker $C(\mathbf{r}, t)$ for a uniform driving with $\phi = -\pi/2$, $\hbar\omega = 7|t_1| > W$, $\Delta_{AB} = 0.1|t_1|$, and $\lambda(t)$ linearly ramped up to $\lambda_f = 1$ in $\tau_{\text{QA}} = 300\tau$, followed by a constant- λ_f evolution for $\tau_f = 220\tau$, with $\tau = 2\pi/\omega$. The topological transition occurs at $\lambda_{\text{cr}} \approx 0.57$. Here, $L = N_x = N_y = 48$, and we average on a central square of size 12×12 . The horizontal line at ≈ 0.96 is the time average $C_{\text{bulk}}^{\text{av}}$, calculated from $t = \tau_{\text{QA}}$ to $t = \tau_{\text{QA}} + \tau_f$. The upper inset shows the saturation of $C_{\text{bulk}}^{\text{av}}(L, \tau_{\text{QA}} \rightarrow \infty)$ to a limiting value that (see the lower inset, where we fit points with standard power-law corrections $1 + c_1/L + c_2/L^2$) goes to 1 for $L \rightarrow \infty$.

of electronic occupations of the states: The final Floquet GS $|\Psi_{\text{FGS}}[\lambda(\tau_{\text{QA}})]\rangle$ is *never* reached, even for $\tau_{\text{QA}} \rightarrow \infty$. The analysis of these issues will be the subject of a future work [38]. Figure 4 shows the final Floquet quasienergy bands, with the corresponding population indicated by a variable-size dot, for $\hbar\omega = 4|t_1| < W$ and $\lambda(t)$ linearly ramped up to $\lambda_f = 1$ in $\tau_{\text{QA}} = 300\tau$. The final state reached is a nonequilibrium metal, rather than an insulator. This aspect is important in devising pump-probe photoemission experiments in graphene [16].

Conclusions. We found a nonequilibrium mechanism which selectively populates edge states when performing an adiabatic switching on of a periodic perturbation towards a topologically nontrivial insulating phase. It is different from the “topological blocking” of Ref. [39], which works with PBCs and when

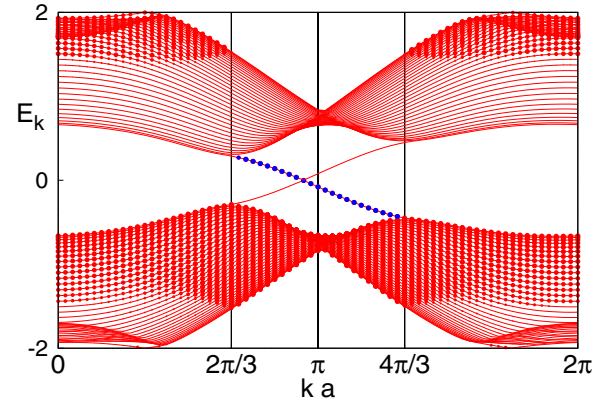


FIG. 4. Final Floquet quasienergies $E_{k,\alpha}$ and occupations $n_{k,\alpha}$ (dot size proportional to $n_{k,\alpha}$) for $\phi = -\pi/2$, $\hbar\omega = 4|t_1| < W$, $\Delta_{AB} = 0.1|t_1|$ (constant), and $\lambda(t)$ linearly ramped up to $\lambda_f = 1$ in $\tau_{\text{QA}} = 300\tau$.

driving systems with symmetry-protected subspaces *from* the topologically nontrivial phase *to* the trivial one. The mechanism we illustrated requires edge states (hence OBC) whose electronic occupation is unable to follow instantaneous equilibrium as they become topologically nontrivial and cross the bulk gap. It is general enough, and is at the root of the deviations from KZ scaling in one-dimensional (1D) topological transitions, as seen in Refs. [40,41]. In the present 2D context, it adds flexibility to the control of the edge currents flowing at the boundaries of the sample, including the ability to have currents flowing only at one edge, by appropriate focusing of the ac field. Finally, we have shown that for $\hbar\omega < W$ intraband resonances ruin the adiabatic picture and the resulting state is a nonequilibrium metal. Our findings should be amenable to experimental tests both with ultracold atoms in optical lattices [1], and with laser-irradiated electronic systems.

Acknowledgments. We acknowledge discussions with I. Carusotto, A. Dutta, R. Fazio, A. Russomanno, A. Silva, and E. Tosatti. Research was supported by MIUR PRIN-2010LLKJBX-001, and by EU ERC MODPHYSFRICT.

-
- [1] G. Jotzu, M. Messer, R. Desbuquois, M. Lebrat, T. Uehlinger, D. Greif, and T. Esslinger, *Nature (London)* **515**, 237 (2014).
- [2] F. D. M. Haldane, *Phys. Rev. Lett.* **61**, 2015 (1988).
- [3] T. Oka and H. Aoki, *Phys. Rev. B* **79**, 081406 (2009).
- [4] J. Cayssol, B. Dóra, F. Simon, and R. Moessner, *Phys. Status Solidi RRL* **7**, 101 (2013).
- [5] T. Kitagawa, E. Berg, M. Rudner, and E. Demler, *Phys. Rev. B* **82**, 235114 (2010).
- [6] H. L. Calvo, H. M. Pastawski, S. Roche, and L. E. F. Torres, *Appl. Phys. Lett.* **98**, 232103 (2011).
- [7] T. Kitagawa, T. Oka, A. Brataas, L. Fu, and E. Demler, *Phys. Rev. B* **84**, 235108 (2011).
- [8] N. H. Lindner, G. Refael, and V. Galitski, *Nat. Phys.* **7**, 490 (2011).
- [9] M. S. Rudner, N. H. Lindner, E. Berg, and M. Levin, *Phys. Rev. X* **3**, 031005 (2013).
- [10] A. Kundu, H. A. Fertig, and B. Seradjeh, *Phys. Rev. Lett.* **113**, 236803 (2014).
- [11] Á. Gómez-León, P. Delplace, and G. Platero, *Phys. Rev. B* **89**, 205408 (2014).
- [12] L. E. F. Foa Torres, P. M. Perez-Piskunow, C. A. Balseiro, and G. Usaj, *Phys. Rev. Lett.* **113**, 266801 (2014).
- [13] A. G. Grushin, Á. Gómez-León, and T. Neupert, *Phys. Rev. Lett.* **112**, 156801 (2014).
- [14] L. D’Alessio and M. Rigol, *Nat. Commun.* **6**, 8336 (2015).
- [15] J. P. Dahlhaus, B. M. Fregoso, and J. E. Moore, *Phys. Rev. Lett.* **114**, 246802 (2015).
- [16] M. Sentef, M. Claassen, A. Kemper, B. Moritz, T. Oka, J. Freericks, and T. Devereaux, *Nat. Commun.* **6**, 7047 (2015).

- [17] P. Titum, N. H. Lindner, M. C. Rechtsman, and G. Refael, *Phys. Rev. Lett.* **114**, 056801 (2015).
- [18] M. D. Caio, N. R. Cooper, and M. J. Bhaseen, *Phys. Rev. Lett.* **115**, 236403 (2015).
- [19] H. Dehghani, T. Oka, and A. Mitra, *Phys. Rev. B* **91**, 155422 (2015).
- [20] H. P. Breuer and M. Holthaus, *Phys. Lett. A* **140**, 507 (1989).
- [21] H. P. Breuer and M. Holthaus, *Z. Phys. D* **11**, 1 (1989).
- [22] T. Kadowaki and H. Nishimori, *Phys. Rev. E* **58**, 5355 (1998).
- [23] G. E. Santoro, R. Martoňák, E. Tosatti, and R. Car, *Science* **295**, 2427 (2002).
- [24] G. E. Santoro and E. Tosatti, *J. Phys. A* **39**, R393 (2006).
- [25] A. Dutta, G. Aeppli, B. K. Chakrabarti, U. Divakaran, T. Rosenbaum, and D. Sen, *Quantum Phase Transitions in Transverse Field Spin Models: From Statistical Physics to Quantum Information* (Cambridge University Press, Cambridge, UK, 2015).
- [26] T. W. B. Kibble, *Phys. Rep.* **67**, 183 (1980).
- [27] W. H. Zurek, *Nature (London)* **317**, 505 (1985).
- [28] W. H. Zurek, *Phys. Rep.* **276**, 177 (1996).
- [29] A. Polkovnikov, K. Sengupta, A. Silva, and M. Vengalattore, *Rev. Mod. Phys.* **83**, 863 (2011).
- [30] L. D. Landau, *Phys. Z. Sowjetunion* **2**, 46 (1932).
- [31] C. Zener, *Proc. R. Soc. London, Ser. A* **137**, 696 (1932).
- [32] R. Bianco and R. Resta, *Phys. Rev. B* **84**, 241106 (2011).
- [33] See Supplemental Material at <http://link.aps.org/supplemental/10.1103/PhysRevB.93.241406> for details on the Schrödinger dynamics implemented, on the calculation of bond currents, and on the local Chern marker.
- [34] J. L. Lado, N. García-Martínez, and J. Fernández-Rossier, *Synth. Met.* **210**, 56 (2015).
- [35] S. C. Althorpe, D. J. Kouri, D. K. Hoffman, and N. Moiseyev, *Chem. Phys.* **217**, 289 (1997).
- [36] D. E. Liu, A. Levchenko, and H. U. Baranger, *Phys. Rev. Lett.* **111**, 047002 (2013).
- [37] R. B. Laughlin, *Phys. Rev. B* **23**, 5632 (1981).
- [38] L. Privitera *et al.* (unpublished).
- [39] G. Kells, D. Sen, J. K. Slingerland, and S. Vishveshwara, *Phys. Rev. B* **89**, 235130 (2014).
- [40] A. Bermudez, L. Amico, and M. A. Martin-Delgado, *New J. Phys.* **12**, 055014 (2010).
- [41] A. Bermudez, D. Patane, L. Amico, and M. A. Martin-Delgado, *Phys. Rev. Lett.* **102**, 135702 (2009).